Cytometry
PART A
Journal of the International Society for Advancement of Cytometry

Stromal Vascular Progenitors in Adult Human Adipose Tissue

Ludovic Zimmerlin,[1,2,3] Vera S. Donnenberg,[2,4] Melanie E. Pfeifer,[1,2] E. Michael Meyer,[2] Bruno Péault,[5] J. Peter Rubin,[4] Albert D. Donnenberg[1,2]*

[1]Department of Medicine, Division of Hematology/Oncology, University of Pittsburgh School of Medicine, Pittsburgh, Pennsylvania

[2]University of Pittsburgh Cancer Institute, Pittsburgh, Pennsylvania

[3]École doctorale Biologie et Biotechnologie, Université Paris Diderot - Paris 7, Paris, France

[4]Department of Surgery, University of Pittsburgh School of Medicine, Pittsburgh, Pennsylvania

[5]University of California at Los Angeles, Department of Orthopedic Surgery, Los Angeles, California

Received 5 August 2009; Revision Received 17 September 2009; Accepted 22 September 2009

Additional Supporting Information may be found in the online version of this article.

Grant sponsor: Production Assistance for Cellular Therapy (PACT); Grant number: N01-HB-37165; Grant sponsor: National Heart, Lung, and Blood Institute; Grant number: R01-HL-085819.

*Correspondence to: Albert D. Donnenberg, Hillman Cancer Center Research Pavilion Suite2.42c, 5117 Center Avenue, Pittsburgh, PA 15213-2582, USA

Email: donnenbergad@upmc.edu

Published online 22 October 2009 in Wiley InterScience (www.interscience.wiley.com)

DOI: 10.1002/cyto.a.20813

Abstract

The in vivo progenitor of culture-expanded mesenchymal-like adipose-derived stem cells (ADSC) remains elusive, owing in part to the complex organization of stromal cells surrounding the small vessels, and the rapidity with which adipose stromal vascular cells adopt a mesenchymal phenotype in vitro. Immunohistostaining of intact adipose tissue was used to identify three markers (CD31, CD34, and CD146), which together unambiguously discriminate histologically distinct inner and outer rings of vessel-associated stromal cells, as well as capillary and small vessel endothelial cells. These markers were used in multiparameter flow cytometry in conjunction with stem/progenitor markers (CD90 and CD117) to further characterize stromal vascular fraction (SVF) subpopulations. Two mesenchymal and two endothelial populations were isolated by high speed flow cytometric sorting, expanded in short term culture, and tested for adipogenesis. The inner layer of stromal cells in contact with small vessel endothelium (pericytes) was CD146+/α-SMA+/CD90±/CD34−/CD31−; the outer adventitial stromal ring (designated supra adventitial-adipose stromal cells, SA-ASC) was CD146−/α-SMA−/CD90+/CD34+/CD31−. Capillary endothelial cells were CD31+/CD34+/CD90+ (endothelial progenitor), whereas small vessel endothelium was CD31+/CD34−/CD90− (endothelial mature). Flow cytometry confirmed these expression patterns and revealed a CD146+/CD90+/CD34+/CD31− pericyte subset that may be transitional between pericytes and SA-ASC. Pericytes had the most potent adipogenic potential, followed by the more numerous SA-ASC. Endothelial populations had significantly reduced adipogenic potential compared with unsorted expanded SVF cells. In adipose tissue, perivascular stromal cells are organized in two discrete layers, the innermost consisting of CD146+/CD34− pericytes, and the outermost of CD146−/CD34+ SA-ASC, both of which have adipogenic potential in culture. A CD146+/CD34+ subset detected by flow cytometry at low frequency suggests a population transitional between pericytes and SA-ASC. © 2009 International Society for Advancement of Cytometry

Key terms

multiparameter flow cytometry; adipose-derived stem cells; adipose derived stromal cells; endothelial cells; perivascular cells; pericytes; immunofluorescence microscopy; supra adventitial-adipose stromal cells

ADIPOSE tissue represents an attractive source of autologous adult stem cells for regenerative therapy due to its abundance, surgical accessibility, and high content of multipotential mesenchymal (1,2) and endothelial (3–5) progenitor cells. Although autologous fat transplantation was reported more than a century ago (6) and adipogenic progenitors were isolated by adherence from the human fat stromal vascular fraction (SVF) in 1976 (7,8), multipotent adipose-derived stem cells (ADSC) were described during the last decade. ADSC mimic in vitro properties of bone marrow-derived mesenchymal stem cells (BM-MSC), expressing similar antigens (1) and differentiating toward all mesenchymal lineages (adipogenic, osteogenic, chondrogenic, myogenic (2), and cardiomyogenic (9)), and beyond (angiogenic (3,4), epithelial

(10), hepatic (11), and neurogenic (12,13)). Like their bone marrow-derived counterparts, ADSC retain their MSC properties after serial passage (14).

Because the definition of ADSC is linked to the in vitro methods used for their isolation (preparation of SVF and selection by outgrowth of plastic adherent cells), attempts to elucidate their in situ identity have yet to be validated and multiple populations have been proposed without full consensus. Although ADSC acquire markers associated with BM-derived MSC during in vitro culture, initial expression levels in the freshly isolated SVF are low (15,16). Vascular associated MSC, dubbed pericytes, were recently proposed to be a resident population in most of tissues of mesodermal origin (17,18), including fat. In vivo these cells appear as CD146+, α-SMA+, and CD34− cells in contact with the intimal surface of small vessels. CD34 is a well known stem cell marker in both hematopoietic (19) and endothelial lineages (20) but is absent on BM-derived MSC (21). In addition to this pericytic layer, the small vessels of adipose tissue are encircled by an outer adventitial ring of CD34+ nonendothelial cells (22–24). While several studies support the expression of pericyte markers by ADSC-generating cells (25,26), several recent publications agree that ADSC are derived from a mutually exclusive CD34+ population (16,23,27). A single study (24) that has been criticized for its conclusions (23) claims coexpression of CD34 and pericyte markers on cultured SVF. This controversy has been further clouded by separation methods relying on a single marker (25,28,29). CD34+ cells isolated from fresh SVF or early passage adherent cells were found to be either enriched (28) or depleted (29) of cells with high adipogenic potential, respectively. Such simplified separation strategies may mask the heterogeneity of the fat SVF, pooling cell populations that occupy discrete anatomical niches.

To overcome the difficulties imposed by the SVF heterogeneity, we developed a multiparameter flow cytometric analytic and sorting strategy which included the hematopoietic markers CD45 and CD3, the endothelial marker CD31, the perivascular marker CD146, and the stem/progenitor markers CD34, CD90, and CD117 (c-Kit). In this study, four distinct vessel-associated cell populations were defined in the nonhematopoietic SVF fraction by three classifier antigens (CD31, CD34, and CD146), which were validated by immunohistostaining of fresh intact adipose tissue. These populations were further characterized for expression of the stem/progenitor related markers CD90 and CD117, sorted, expanded, and assayed for adipogenic potential.

Methods

Tissue Collection

Subcutaneous adipose tissue was harvested during elective abdominoplasty from human adult female patients at Magee Womens Hospital. All samples were waste materials collected as a byproduct of surgery. Deidentified samples were collected under an IRB approved exemption (number 0511186, University of Pittsburgh IRB). Samples were immediately transported to the laboratory and processed on receipt.

Flow Cytometry and Cell Sorting

Fat tissue was thoroughly minced with scissors, digested for 30 min in Hanks' Balanced Salt Solution (HBSS, Invitrogen, Carlsbad, CA) containing 3.5% Bovine Serum Albumin (BSA, Millipore, Charlottesville, VA) and 1 mg/mL collagenase type II (Worthington, Lakewood, NJ) on a shaking water bath at 37°C, and finally disaggregated through successive 425 μm and 180 μm sieves (W.S. Tyler, Mentor, OH). Mature adipocytes were eliminated by centrifugation (400*g*, ambient temperature, 10 min) and cell pellets were resuspended in NH_4Cl-based erythrocyte lysis buffer (Beckman Coulter, Miami, FL, Cat No. IM3630d), incubated for 10 min at room temperature (RT) and washed in Phosphate Buffer Saline (PBS). Viable cell enrichment and debris depletion was achieved on a Ficoll-Hypaque density gradient (Histopaque®-1077, Sigma-Aldrich, St. Louis, MO). Cell suspensions were deposited on slides using a Cytospin-2 cytocentrifuge (Thermo Shandon, Pittsburgh, PA) and Wright-Giemsa stained (Wright Giemsa Stain Hematology Stain Pack, Fisher Diagnostics, Fisher Scientific, Middletown, VA) with an Ames Hema-tek stainer and photographed under bright-field microscopy using a digital camera and software (Spot Insight 2 Meg FW Color Mosaic model 18.2, Diagnostic Instruments) interfaced to a Nikon Labophot microscope.

Freshly isolated cells from the SVF were maintained from then on ice and stained for analytical flow cytometry and cell sorting experiments as previously described (30). Cell suspensions were centrifuged (200*g*, 7 min) and the cell pellet was preincubated with 5 μL neat mouse serum (Sigma) to minimize nonspecific antibody binding. Cells were simultaneously stained with monoclonal mouse anti-human fluorochrome-conjugated antibodies (2 μL each, CD3-FITC, CD146-PE, CD34-ECD, CD90-PE-Cy5, and CD117-PE-Cy7, all Beckman Coulter, CD31-APC, and CD45-APC-Cy7, BD Biosciences, San Jose, CA).

Analytical samples were fixed with 2% methanol-free formaldehyde (Polysciences, Warrington, PA), permeabilized in PBS with 0.1% saponin (Coulter), 0.5% BSA for 10 min at RT, and incubated with 7.7 μg/mL 4′,6-diamidino-2-phenylindole (DAPI, Invitrogen). Eight-color, 14-parameter data files were acquired on a three-laser CyAn ADP cytometer (Beckman Coulter) at a maximum of 10,000 events per second. Up to 10,000,000 events were acquired per sample. The DAPI signal was acquired independently on both logarithmic and linear (for cell cycle analysis) scales by optimizing voltage and gain settings of two individual photomultiplier tubes (PMT). For compensation purposes, BD Calibrite™ beads (BD Biosciences) and single antibody-stained mouse IgG capture beads (BD Biosciences) were acquired for single fluorochromes (FITC, PE, APC) and tandem-dyes (ECD, PE-Cy5, PE-Cy7, and APC-Cy7), respectively. Initially, regions and gates were set with the aid of "fluorescence minus outcomes" isotype controls. An annotated example is given in the supporting information associated with the on-line version of this article. Offline compensation and analysis were performed using the high throughput parallel processing VenturiOne software (Applied Cytometry, Sheffield, UK). Ten independent

samples were analyzed. Summarized results are given as arithmetic means ± SEM, where mean values are compared, and ± SD where sample to sample variability is characterized (31).

Cell sorting was performed using a three-laser MoFlo high speed cell sorter (Beckman Coulter) equipped with a class I biosafety cabinet.

Unfixed eight-color stained samples were suspended in PBS, 2 mM ethylenediaminetetraacetic acid (EDTA, Sigma), 0.5% BSA, supplemented with 2 μg/mL DAPI for exclusion of dead and apoptotic cells. Samples were continuously cooled to 4°C and four-way sorting was performed at 10,000-to-20,000 events per second. Samples were collected into sterile polypropylene tubes containing 500 μL fetal calf serum (FCS, Atlanta Biologicals, Lawrenceville, GA) and plated in uncoated BD Falcon™ plates/flasks (BD Biosciences) at a density of 10,000 to 25,000 cells per cm^2. Adherent sorted and unsorted cells were expanded in equal volumes of Dulbecco's Modified Eagle Medium/Nutrient Mixture F-12 (DMEM/F12) + DMEM (Invitrogen) and supplemented with 10% FCS, 0.1 μM dexamethasone (Sigma), 100 U/mL penicillin (Sigma), 50 μg/mL gentamycin sulfate (Sigma).

Immunohistochemistry—Immunofluorescence

Small (~1 cm^3) pieces of freshly harvested adipose tissue were washed in PBS, 15% sucrose, immersed in 7.5% gelatin (Sigma) in PBS, 15% sucrose (Sigma), and held for at least 2 h at 4°C, before being frozen by repetitive immersion in liquid nitrogen-cooled 2-methylbutane (Fisher Scientific, Fair Lawn, NJ). Sections (6 to 8 μm) were cut on a Microm cryostat, fixed for 5 min in ice cold acetone (Fisher Scientific), and then stored at −80°C. Before staining, sections were dried at RT and postfixed for 5 min in ice cold acetone. Tissue rehydratation and all subsequent washes were performed by two 5-min incubations in Dako Wash Buffer (Dako, Carpinteria, CA). All incubations were completed at ambient temperature.

For immunohistochemistry experiments, endogenous peroxidase activity was neutralized with Dual Endogenous Enzyme Block solution (Dako) for 10 min. Specimens were washed and nonspecific secondary antibody binding was prevented by a 1 h incubation with PBS, 5% goat serum (Sigma), 0.05% Tween20 (Dako). Sections were incubated with prediluted uncoupled mouse anti-human antibodies for 1 h. Dako Universal Mouse Negative Control (Dako) was substituted for primary antibodies for a negative control. Specimens were washed and incubated for 30 min with horseradish-peroxidase (HRP)-labeled polymers (Dako Envision$^+$ Dual Link System-HRP, Dako). Staining was completed by incubating the rinsed specimens with 3,3′-diaminobenzidine (DAB+) substrate-chromogen (Dako) for 1 to 3 min. Finally, tissue sections were washed in Dako Wash Buffer, stained for 3 min with Hematoxylin (Dako), and rinsed in deionized water. Dehydrated specimens were mounted in nonaqueous medium (Cytoseal™280, Richard-Allan Scientific, Kalamazoo, MI) and photographed under bright-field microscopy using a Spot Insight 2Meg FW Color Mosaic digital camera (Diagnostic Instruments).

For fluorescent immunostaining, rehydrated tissue sections were pretreated with goat serum blocking solution and incubated with primary unconjugated antibodies for 1 h. Washed sections were sequentially incubated for 1 h with biotinylated secondary goat anti-mouse antibody (Dako) and for 30 min with streptavidin-Cy3 (Sigma). Nuclear staining was attained through 5-min incubation with (300 nM) DAPI (Invitrogen). Slides were mounted in 1:1 PBS/glycerol (Sigma) or Prolong Gold anti-fade reagent (Invitrogen) and observed under an epi-fluorescence microscope (Nikon Eclipse TE 2000-U).

Primary antibodies used in these studies were anti-CD31 (ready-to-use, Dako, Cat No. N1596 and 1:50, SantaCruz Biotechnology, Santa Cruz, CA, Cat No. SC13537 for immunohistochemistry and immunofluorescence experiments, respectively), anti-CD34 (1:50, BD Biosciences, Cat No. 347660), anti-CD90 (1:100, BD Biosciences, Cat No. 550402), anti-CD146-FITC (1:20, AbD Serotec, Raleigh, NC, Cat No. MCA2141F), and anti-α-SMA-FITC (1:200, Sigma, Cat No. F3777). All antibodies and streptavidin-Cy3 were diluted in PBS, 5% goat serum, 0.05% Tween20.

Adipogenic Differentiation and Oil Red O Staining

For adipogenic differentiation, expanded adherent cells were trypsinized (5 min incubation with 0.25% Trypsin/EDTA, Cellgro, Mediatech, Manassas, VA) and transferred into replicate (4,5) 24-well plates (50,000 cells/well) and allowed to adhere overnight. Culture medium was supplemented with 1 μM dexamethasone, 0.5 μM isobutylmethylxantine, 60 μM indomethacin, and 10 μg/mL insulin (all Sigma). After 21 days, cells were fixed in 2% formaldehyde (Polysciences, Inc.) in PBS for 15 min at room temperature. Fixed cells were washed in 60% isopropanol and stained for 10 min with Oil Red O (Sigma) at RT. After five consecutive washes in deionized water, the presence of red stained lipid was documented using bright-field microscopy. The number of cells per low power field (10× objective, five–eight fields) with at least five large Oil Red O+ vesicles was recorded for each culture. For cells derived from each sorted population, Student's paired two tailed *t*-test was performed comparing the $\log_{10}$ of Oil Red O+ cells derived from each fraction to the $\log_{10}$ of Oil Red O+ cells in unsorted cells from the same experiment. Since the difference of logs is equivalent to a ratio in the arithmetic domain, this statistic provided a convenient assessment of adipogenic potential relative to unsorted cells.

Results

Validation of Sort Classifiers Based on In Situ Immunohistostaining of the Fat Vasculature

White adipose tissue is richly vascularized (Fig. 1a). After dissociation, elimination of mature adipocytes by centrifugation and isolation of mononuclear cells by Ficoll-Hypaque gradient, the stromal vascular fraction (SVF) of fat tissue remains highly heterogeneous (Fig. 1b). To design our flow cytometric gating strategy, it was necessary to select reliable markers capable of classifying cells into distinct cell

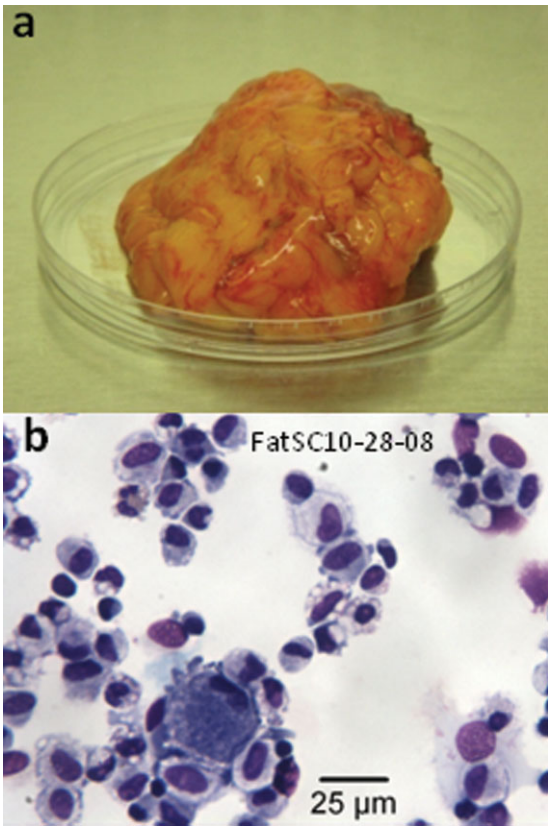

Figure 1. (**a**) Unmanipulated fat tissue (~50 g) upon accession after surgery. (**b**) Cytocentrifuge preparation of the dissociated fat SVF after erythrocyte lysis and Ficoll-Hypaque separation (Giemsa-Wright staining, ×40 objective). [Color figure can be viewed in the online issue, which is available at www.interscience.wiley.com.]

populations within the adipose stromal vascular fraction. We investigated the immunolocalization of known endothelial and perivascular markers including CD31, CD34, CD90, CD146, and α-SMA, in situ in cryosections of human fat (Fig. 2). CD31 was expressed at the luminal cell layer of small vessels and on capillaries and marked a population distinct from perivascular α-SMA+ cells (Fig. 2, top row). CD34 is a known endothelial marker (32) which is also expressed by both hematopoietic (19) and endothelial (20) progenitor cells. CD34 was expressed on two distinct layers in both arterioles and venules. It was dimly expressed by luminal endothelial cells but visualized as brightly staining cells in the adventitia of blood vessels (Fig. 2, middle row). CD34 expression was higher on the endothelial cells of capillaries than on those of small vessels. On the basis of these observations, we selected CD31 to identify vascular endothelial cells, whereas the intensity of CD34 expression was used to determine whether CD31+ cells were derived from capillaries or larger vessels. CD146 proved to be a reliable marker for adventitial perivascular cells immediately adjacent to the vascular intima (pericytes), but, unlike α-SMA, it was also detected on endothelial cells. In our immunohistostaining, CD34 and CD146 appeared to mark distinct populations (Fig. 2, middle row). Although α-SMA helped us positively identify pericytes in immunohistostaining, the fact that it is an intracellular marker rules out its use for identifying and sorting viable cells by flow cytometry. We, therefore, validated the membrane associated adhesion molecule CD146 to identify pericytes among CD31-negative nonendothelial cells. Similarly, CD34 staining was used to identify nonendothelial, nonpericytic (CD31 and CD146 double negative) cells visualized in an outer ring adjacent to the adventitial pericytes (here designated supra adventitial-adipose stromal cells, SA-ASC). CD90 is an established stem cell marker in the hematopoietic system (33,34) and in mesenchymal stem cells (35,36) and was also shown to be expressed on some endothelial (37,38) and smooth muscle (39) cells. CD90 expression was detected on the endothelium of capillaries but not small vessels (Fig. 2, bottom row), where CD90 was predominantly expressed in the outer supra adventitial ring.

Flow Cytometry Gating Strategy: Exclusion of Sources of Artifact

Flow cytometry has the advantage of increased sensitivity and dynamic range compared with microscopy. Additionally, millions of cells can be assayed in each sample, allowing the detection of rare populations that cannot be resolved by microscopy. However, disaggregated adipose tissue contains cells and debris that can interfere with flow cytometry and lead to erroneous conclusions. To develop our gating strategy, we analyzed 10 independent samples of abdominal fat stromal vascular cells (300,998 to 10,000,000 events per sample). A representative sample is shown in Figure 3. Forward Scatter (FS) pulse analysis permits elimination of cell doublets and clusters present in tissue digests, preventing the false association of markers present on distinct populations (selection of singlets, region A). The nuclear dye DAPI was used after gentle permeabilization to discriminate diploid cells from anucleate events (such as lipid droplets) and hypodiploid apoptotic cells (selection of nucleated events, region B). We used the light scatter properties of CD45+ CD3+ T lymphocytes (color-evented red), a small resting cell population, as an internal standard to guide in the elimination of low light scatter debris (region C). A compound gate including only events within gates A, B, and C for further analysis excluded 54.7 ± 17.7% (mean ± SD) of events as artifactual (Table 1). Although these three regions allowed us to select cellular nucleated singlets, highly autofluorescent cells were still detected in the three first channels excited by the blue laser, as revealed by the presence of diagonal streaks in 2-parameter histograms (Fig. 3, left box, middle row). Events were considered autofluorescent if they fell within gates D and E and F and were eliminated from further analysis. The remaining events were considered nucleated singlet cells and were used as the denominator for the analysis (Table 1). Finally, hematopoietic cells as well as cells nonspecifically binding murine antibody were eliminated using CD45 and CD3 (left box, top). On average, the hematopoietic fraction accounted for 19.2 ± 7.7% of nucleated cells, suggesting that these cells were preferentially recovered after tissue disaggregation. Importantly, 70.0 ± 13.3% of acquired events

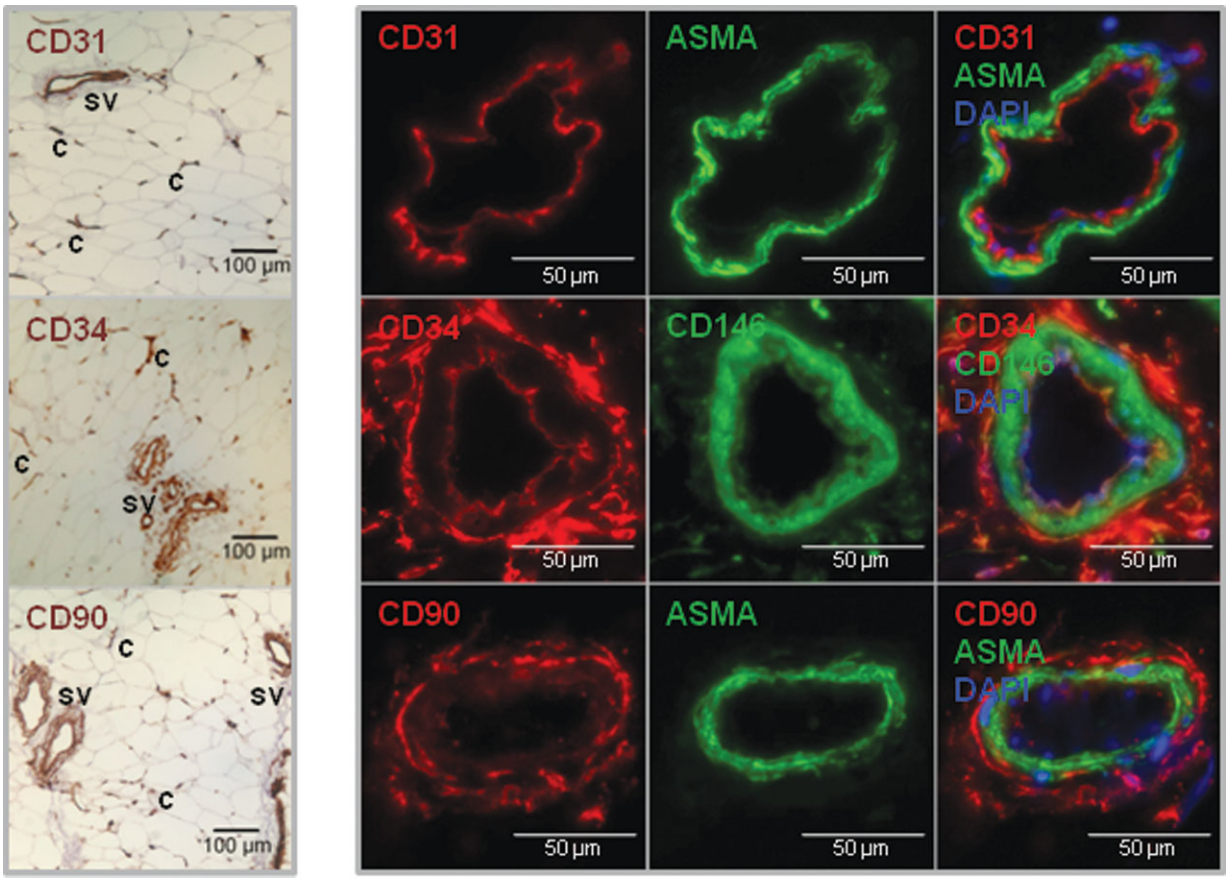

Figure 2. Immunohistostaining of endothelial and perivascular markers in human subcutaneous fat tissue. Immunohistochemistry (left column, ×10 objective) and immunofluorescence (right panel, from left to right, Cy3 staining, FITC staining, Cy3, FITC and DAPI merged, ×40 objective). Top row: CD31 staining was exclusively visualized at the luminal surface of small blood vessels (sv) and capillaries (c). Costaining with the perivascular marker ASMA confirmed the endothelial specificity of anti-CD31 staining. Middle row: CD34 staining was visualized on capillaries (c) and on two distinct layers of the vessel wall of arterioles and venules (sv). CD34 staining was dim on the luminal endothelium and bright in the supra-adventitial layer. While CD146 was detected mostly on perivascular cells, endothelial staining was also observed. Coexpression of CD34 and CD146 was not detected by immunohistostaining. Bottom row: CD90 staining was also observed on capillaries and small vessels. While CD90 stained endothelial cells on capillaries (c, immunofluorescence not shown), its expression was predominantly supra-adventitial, similar to the outer ring of CD34 positive cells. These data are the most informative of five consistent independent experiments.

were eliminated as sources of artifact or irrelevant hematopoietic cells before the analysis of adipose stromal vascular cells (Table 1).

Characterization of the Fat Stromal Vascular Fraction by Analytical Flow Cytometry

Following elimination of interfering events and hematopoietic cells, we proceeded to analyze the samples for the presence of the classifying markers determined by immunohistostaining (CD146, CD34, and CD31). Expression of the stem cell associated markers CD90 and CD117 (c-Kit) was evaluated on the populations defined by the classifying markers (Table 2). Among nonhematopoietic CD45− cells, endothelial cells were identified by CD31 expression and, in agreement with microscopic evaluation, comprised two distinct populations based on CD34 expression. CD31+/CD34^{bright}/CD45− cells, corresponding to capillary endothelial cells were most prevalent and were tentatively named "endothelial progenitors," whereas the minor complementary CD31+/CD34−/CD45− endothelial population, most likely derived from larger vessels, was designated "endothelial mature." In addition to CD34 expression, endothelial progenitors were characterized by a greater proportion of CD90+ cells than endothelial mature cells (mean ± SEM, 91.2 ± 3.4% versus 36.6 ± 9.5%, respectively), consistent with the idea that they represent a more primitive population. Both endothelial populations contained subsets of CD146+ cells at similar levels (15.2 ± 4.8% and 17.0 ± 5.5%, respectively). Pericytes were defined as CD146+ nonendothelial cells (CD146+/CD31−/CD45−, 2.7 ± 1.8% of nonheme cells) and included a substantial subset of CD90+ cells (Table 2). In contrast to our single marker immunohistochemical studies, nearly a third of pericytes coexpressed CD34 and CD90, again suggesting a primitive population. This definition of pericytes excluded a 20-fold

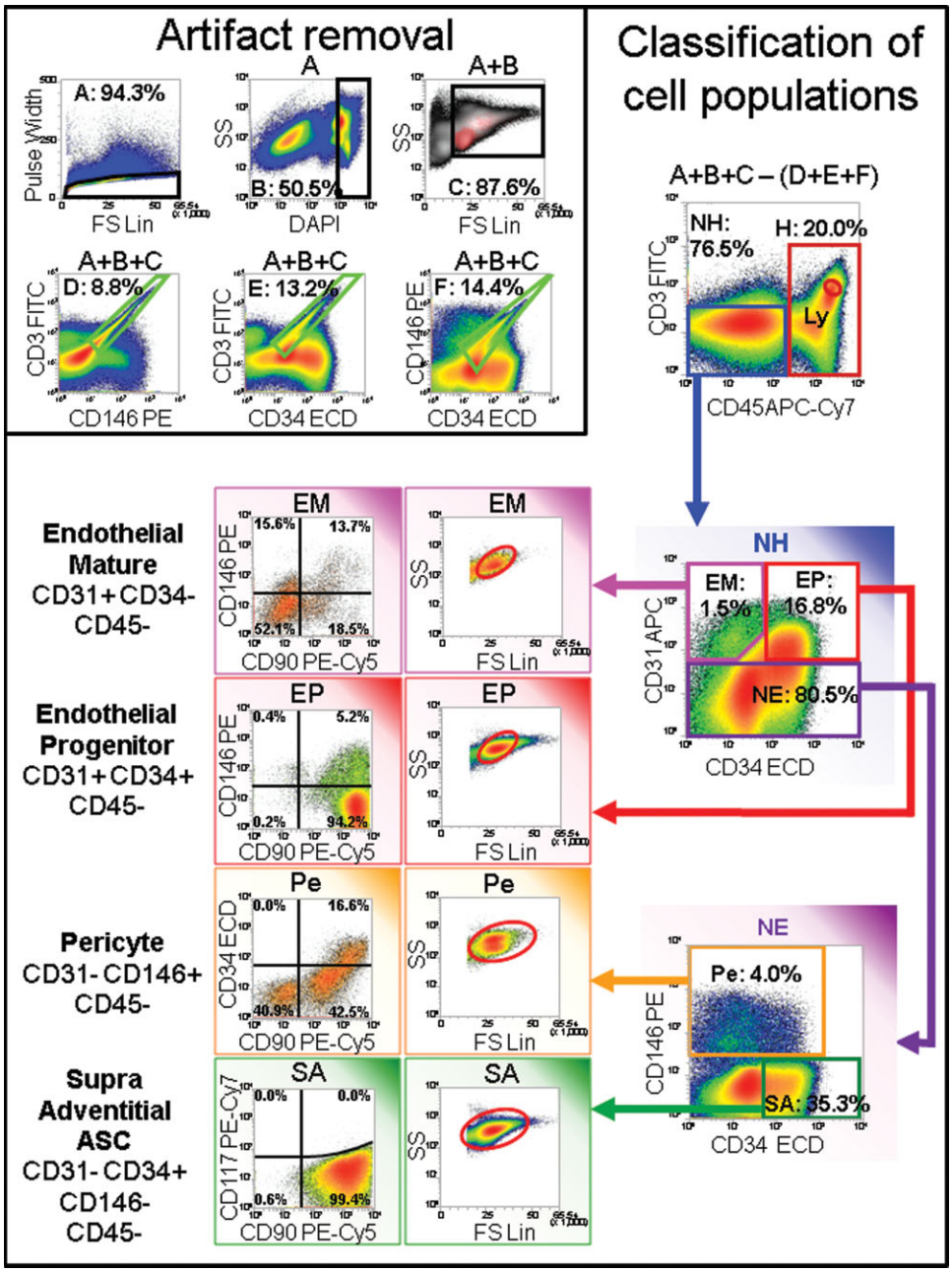

Figure 3. Classification of endothelial and perivascular populations for analytical flow cytometry. Top left box, upper row: Identification of singlet cells with DNA content $\geq$ 2 N. FS pulse analysis was used to remove cell clumps remaining after disaggregation (**A**). Cells were gently permeabilized after fixation, permitting DAPI-dim hypodiploid events to be eliminated for the analytical population (**B**). Events with low light scatter were eliminated (**C**) on the basis of the location of small resting T lymphocytes (CD3+CD45+ lymphocytes (Ly), color evented red). Top left box, lower row: Elimination of autofluorescent events. Cells with high autofluorescence form a diagonal streak in 2-parameter histograms of the first three fluorescence channels. Events present in the compound gate of **D** and **E** and **F** were removed from analysis. In this sample, autofluorescent cells accounted for 8.1% of otherwise analyzable events. Right and bottom panel, top to bottom: Classification of analyzable events into nonhematopoietic (NH) and hematopoietic (H), and nonhematopoietic endothelial (EM, EP) and nonendothelial (NE) populations. Within the endothelial mature subset (EM, pink) the majority of cells were CD90−, with some cells expressing CD146 and dim CD90. Endothelial progenitors (red) were exclusively CD90-bright with heterogeneous CD146 staining. A small proportion of CD90+ cells had saturating fluorescence and were eliminated from the analysis, not shown. Pericytes (Pe, orange) were defined among nonendothelial cells as CD146+, with a subset of bright CD90 cells. A proportion of these CD90+ pericytes coexpressed CD34. SA-ASC (SA, green) were defined among nonendothelial cells as CD34+ CD146− cells. Like endothelial progenitors, the majority of SA-ASC coexpressed bright CD90. No CD117 expression could be detected on SA-ASC and other sorted nonhematopoietic populations as well (not shown). Light scatter profiles are presented for each candidate population. The region percentages represent the proportion of cells within each respective histogram.

Table 1. Removal of sources of artifact and irrelevant cells before analysis of stromal vascular cells

% OF TOTAL EVENTS	MEAN %	SD
Excluded by gates A, B and C	54.7	17.7
Excluded as autofluorescent	8.4	5.6
Excluded as Heme+	6.9	3.4
Total % excluded	70.0	13.3

more prevalent population, which by their phenotype (CD34+/CD31−/CD146−/CD45−) can be identified with the cells that comprise the supra-adventitial ring (SA-ASC). Most SA-ASC were CD90+ (Table 2). The stem cell factor receptor CD117 was not detected on nonhematopoietic populations, but constituted a clear subset of CD45+ cells (not shown), consistent with mast cells (40).

Isolation of Stromal Vascular Populations

We adapted our analytical gating strategy for sorting on an eight-color MoFlo legacy cell sorter. As in our analytical approach, forward scatter pulse height and side scatter analyses were performed to exclude cell clusters. Since cells could not be permeabilized, exclusion of the DNA stain DAPI was used to identify viable cellular events. We relied on a CD3-FITC dump gate to exclude autofluorescent events and CD45 to eliminate hematopoietic cells. Among CD45- nonhematopoietic cells, we were able to detect all four stromal vascular populations: endothelial mature, endothelial progenitor, pericyte, and supra adventitial ASC populations. Populations were simultaneously sorted for functional characterization at a rate of 10,000 to 12,000 events per second with a sort purity of ∼95%.

Adipogenic Potential of Sorted Cells

We successfully expanded in vitro all sorted populations from three independent samples, in parallel with unsorted cells as a control. Adipogenic differentiation was investigated for each population in parallel and all populations showed abilities at various levels to give rise to differentiated progeny which accumulated lipid vesicles as revealed by Oil Red O staining (Fig. 4). As expected, the cells expanded from both endothelial populations were less efficient at adipogenesis than those expanded from unsorted stromal vascular cells. Among the sorted populations, only pericytes gave rise to fat cells with greater efficiency than unsorted cells, indicating that CD45−/CD31−/CD146−/CD34+ supra adventitial ASC may represent a more specialized pericyte-derived population.

Discussion

Our studies relied on histological staining to develop an eight-color flow cytometric analysis and sorting strategy capable of resolving four histologically discrete subpopulations of the adipose SVF. Uniquely among flow cytometric studies reported on adipose-derived cells, we took great care to remove potential sources of artifact such as cell doublets, autofluorescence, debris, and apoptotic cells (41). Four populations were then identified, sorted, expanded in short term culture, and tested for adipogenesis.

Two vascular endothelial populations were defined on the basis of CD31 and CD34 expression. Nonhematopoietic cells coexpressing CD31 and CD34 (endothelial progenitor), the more prevalent of the two, were located within capillaries, whereas CD31+/CD34− cells (endothelial mature) were localized to the lumen of small vessels. The phenotype of adipose derived endothelial progenitors is consistent with that reported for both bone marrow and circulating endothelial progenitor cells (CD45−/CD34+/VEGFR2+, reviewed in Ref. 42, but the frequency in adipose SVF was three to five orders of magnitude higher, making them excellent candidates for regenerative therapy. Pericytes were defined as CD45−/CD31−/CD146+. Since flow cytometry consistently revealed a subset of CD31−/CD146+ cells coexpressing CD34 and CD90, absence of CD34 was purposely omitted from the pericyte definition, in contrast to common practice (16,18,43). Although not easily visualized by immunohistostaining, CD31−/CD146+/CD34+ cells accounted for 0.54 ± 0.50% (mean, SD) of nucleated SVF cells and may comprise a transitional population between the pericytic and supra-adventitial perivascular rings. We designated CD45−/CD31−/CD34+/CD146− cells (>90% CD90+), which localized to the outer vascular ring, supra adventitial-adipose stromal cells (SA-ASC). This population corresponds to Yoshimura's less

Table 2. Quantification of four major populations and their subsets within the stromal vascular fraction of disaggregated adipose tissue

	CD3-CD45-CD31+CD34− ENDOTHELIAL MATURE			CD3-CD45-CD31+CD34+ ENDOTHELIAL PROGENITOR			CD3-CD45-CD31-CD146+ PERICYTE			CD3-CD45-CD31-CD34+ CD146- SA-ASC		
	MEAN	SD	SEM	MEAN	SD	SEM	MEAN	SD	SEM	MEAN	SD	SEM
% of Nucleated cells	2.5	2.7	0.8	13.7	8.3	2.6	1.41	0.97	0.31	27.9	16.5	5.2
% of Nonheme SVF	4.9	4.9	1.5	26.6	16.2	5.1	2.7	1.8	0.6	52.3	24.4	7.7
% Expressing CD34	0	–	–	100	–	–	31.5	17.8	5.6	100	–	–
% Expressing CD90	36.6	30.2	9.5	91.3	10.8	3.4	51.1	19.7	6.2	89.0	9.9	3.1
% Expressing CD90 and CD34	0	–	–				28.3	15.2	4.8			
% Expressing CD146	17.0	17.2	5.4	15.2	15.2	4.8	100	–	–	0	–	–
% Expressing CD117	0.1	0.1	0.0	0.5	1.4	0.4	0.1	0.1	0.0	0.0	0.0	0.0

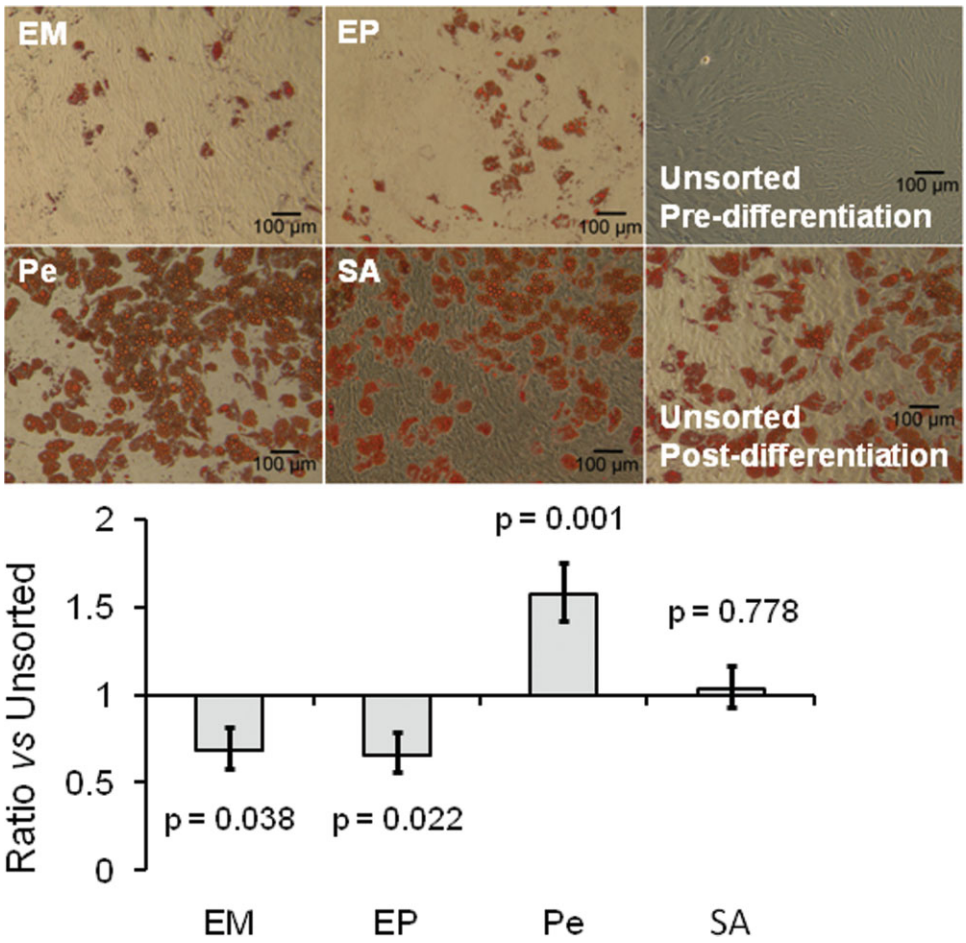

Figure 4. Adipogenic potential from sorted SVF populations. The four candidate progenitor cell populations were simultaneously sorted. Sorted cells were briefly expanded in vitro (one to two passages) prior to transfer to adipogenic conditions. Unsorted ADSC were treated in parallel as a control. Top panels: All populations were able to differentiate toward the adipogenic lineage, giving rise to a differentiated progeny which accumulated lipid vesicles (EM, endothelial mature, EP, endothelial progenitors, Pe, pericytes, SA, SA-ASC). No lipid vesicles were identified prior to exposure to adipogenic conditions. A paired *t*-test was performed comparing the log count of adipocytes in each fraction to its unsorted control. The corresponding differences of log values (ratios) are graphed in the bottom panel with associated *P*-values (two tailed test). Error bars represent the SEM. [Color figure can be viewed in the online issue, which is available at www.interscience.wiley.com.]

descriptive "adipose-derived stromal (or stem) cells [sic] (ASC)" (16).

Experiments performed on sorted SVF were limited by the frequency of CD45−/CD31−/CD146+ pericytes, the rarest population of sorted cells (1.41 ± 0.97% of SVF cells). For this reason, sorted cells were briefly expanded (one to two passages) in the presence of low dose dexamethasone (44,45) which promoted the growth of all populations but did not drive adipogenesis. Alone among the sorted populations, expanded pericytes gave rise to Oil Red O+ fat cells with greater efficiency than unsorted cells. Expanded SA-ASC, the most prevalent sorted population, retained adipogenic potential equivalent to expanded unsorted SVF, whereas both endothelial fractions were relatively depleted of adipogenic cells (Fig. 4). The molecular interactions and signaling pathways that drive adipose progenitor cells (pericytes, SA-ASC) to differentiate into mature adipocytes is an area of active investigation in our (JPR's) laboratory. On the basis of preliminary data, we speculate that downregulation of the Wnt-signaling pathway may play a critical role in driving adipogenic differentiation.

That the two endothelial populations gave rise to lipid positive cells at all may alternatively be explained by plasticity or the outgrowth of contaminating adipogenic cells during the short expansion phase of the experiment. We favor the later interpretation since endothelial cells have been shown to promote the survival of adipogenic cells (46,47) and may have sustained a very small adipogenic contaminant if present. Although we could not directly assess sort purity on the rare populations, reacquiring sorted SA-ASC gave a sort purity of 96.7%.

The adipogenic and chondrogenic potential of pericytes is well established (18,48). Taken together, our study has refined the definition of adipose resident pericytes and shown that both pericytes and the histologically and phenotypically distinct SA-ASC population are capable of adipogenesis after

brief expansion in culture. Although pericytes are the more potent, SA-ASC are the more prevalent. Additionally, we propose that a CD34+/CD90+ subset of pericytes may represent a transitional population between previously reported CD34− pericytes and CD34+ SA-ASC.

Literature Cited

1. Gronthos S, Franklin DM, Leddy HA, Robey PG, Storms RW, Gimble JM. Surface protein characterization of human adipose tissue-derived stromal cells. J Cell Physiol 2001;189:54–63.
2. Zuk PA, Zhu M, Mizuno H, Huang J, Futrell JW, Katz AJ, Benhaim P, Lorenz HP, Hedrick MH. Multilineage cells from human adipose tissue: Implications for cell-based therapies. Tissue Eng 2001;7:211–228.
3. Miranville A, Heeschen C, Sengenes C, Curat CA, Busse R, Bouloumie A. Improvement of postnatal neovascularization by human adipose tissue-derived stem cells. Circulation 2004;110:349–355.
4. Planat-Benard V, Silvestre JS, Cousin B, Andre M, Nibbelink M, Tamarat R, Clergue M, Manneville C, Saillan-Barreau C, Duriez M, Tedgui A, Levy B, Penicaud L, Casteilla L. Plasticity of human adipose lineage cells toward endothelial cells: Physiological and therapeutic perspectives. Circulation 2004;109:656–663.
5. Cao Y, Sun Z, Liao L, Meng Y, Han Q, Zhao RC. Human adipose tissue-derived stem cells differentiate into endothelial cells in vitro and improve postnatal neovascularization in vivo. Biochem Biophys Res Commun 2005;332:370–379.
6. Neuber GA. Fettransplantation. Chir Kongr Verhandl Deutsche Gesellschaft für Chirurgie 1893;22:66.
7. Van RL, Bayliss CE, Roncari DA. Cytological and enzymological characterization of adult human adipocyte precursors in culture. J Clin Invest 1976;58:699–704.
8. Dardick I, Poznanski WJ, Waheed I, Setterfield G. Ultrastructural observations on differentiating human preadipocytes cultured in vitro. Tissue Cell 1976;8:561–571.
9. Planat-Benard V, Menard C, Andre M, Puceat M, Perez A, Garcia-Verdugo JM, Penicaud L, Casteilla L. Spontaneous cardiomyocyte differentiation from adipose tissue stroma cells. Circ Res 2004;94:223–229.
10. Brzoska M, Geiger H, Gauer S, Baer P. Epithelial differentiation of human adipose tissue-derived adult stem cells. Biochem Biophys Res Commun 2005;330:142–150.
11. Seo MJ, Suh SY, Bae YC, Jung JS. Differentiation of human adipose stromal cells into hepatic lineage in vitro and in vivo. Biochem Biophys Res Commun 2005;328:258–264.
12. Zuk PA, Zhu M, Ashjian P, De Ugarte DA, Huang JI, Mizuno H, Alfonso ZC, Fraser JK, Benhaim P, Hedrick MH. Human adipose tissue is a source of multipotent stem cells. Mol Biol Cell 2002;13:4279–4295.
13. Safford KM, Hicok KC, Safford SD, Halvorsen YD, Wilkison WO, Gimble JM, Rice HE. Neurogenic differentiation of murine and human adipose-derived stromal cells. Biochem Biophys Res Commun 2002;294:371–379.
14. Zhu Y, Liu T, Song K, Fan X, Ma X, Cui Z. Adipose-derived stem cell: A better stem cell than BMSC. Cell Biochem Funct 2008;26:664–675.
15. Mitchell JB, McIntosh K, Zvonic S, Garrett S, Floyd ZE, Kloster A, Di Halvorsen Y, Storms RW, Goh B, Kilroy G, Wu X, Gimble JM. Immunophenotype of human adipose-derived cells: Temporal changes in stromal-associated and stem cell-associated markers. Stem Cells 2006;24:376–385.
16. Yoshimura K, Shigeura T, Matsumoto D, Sato T, Takaki Y, Aiba-Kojima E, Sato K, Inoue K, Nagase T, Koshima I, Gonda K. Characterization of freshly isolated and cultured cells derived from the fatty and fluid portions of liposuction aspirates. J Cell Physiol 2006;208:64–76.
17. Covas DT, Panepucci RA, Fontes AM, Silva WA Jr, Orellana MD, Freitas MC, Neder L, Santos AR, Peres LC, Jamur MC, Zago MA. Multipotent mesenchymal stromal cells obtained from diverse human tissues share functional properties and gene-expression profile with CD146+ perivascular cells and fibroblasts. Exp Hematol 2008;36:642–654.
18. Crisan M, Yap S, Casteilla L, Chen CW, Corselli M, Park TS, Andriolo G, Sun B, Zheng B, Zhang L, Norotte C, Teng PN, Traas J, Schugar R, Deasy BM, Badylak S, Buhring HJ, Giacobino JP, Lazzari L, Huard J, Peault B. A perivascular origin for mesenchymal stem cells in multiple human organs. Cell Stem Cell 2008;3:301–313.
19. Civin CI, Strauss LC, Brovall C, Fackler MJ, Schwartz JF, Shaper JH. Antigenic analysis of hematopoiesis. III. A hematopoietic progenitor cell surface antigen defined by a monoclonal antibody raised against KG-1a cells. J Immunol 1984;133:157–165.
20. Asahara T, Murohara T, Sullivan A, Silver M, van der Zee R, Li T, Witzenbichler B, Schatteman G, Isner JM. Isolation of putative progenitor endothelial cells for angiogenesis. Science 1997;275:964–967.
21. Pittenger MF, Mackay AM, Beck SC, Jaiswal RK, Douglas R, Mosca JD, Moorman MA, Simonetti DW, Craig S, Marshak DR. Multilineage potential of adult human mesenchymal stem cells. Science 1999;284:143–147.
22. Pusztaszeri MP, Seelentag W, Bosman FT. Immunohistochemical expression of endothelial markers CD31. CD34, von Willebrand factor, and Fli-1 in normal human tissues. J Histochem Cytochem 2006;54:385–395.
23. Lin G, Garcia M, Ning H, Banie L, Guo YL, Lue TF, Lin CS. Defining stem and progenitor cells within adipose tissue. Stem Cells Dev 2008;17:1053–1063.
24. Traktuev DO, Merfeld-Clauss S, Li J, Kolonin M, Arap W, Pasqualini R, Johnstone BH, March KL, Traktuev DO, Merfeld-Clauss S, Li J, Kolonin M, Arap W, Pasqualini R, Johnstone BH, March KL. A population of multipotent CD34-positive adipose stromal cells share pericyte and mesenchymal surface markers, reside in a perienthelial location, and stabilize endothelial networks. Circ Res 2008;102:77–85.
25. Zannettino AC, Paton S, Arthur A, Khor F, Itescu S, Gimble JM, Gronthos S. Multipotential human adipose-derived stromal stem cells exhibit a perivascular phenotype in vitro and in vivo. J Cell Physiol 2008;214:413–421.
26. Khan WS, Tew SR, Adesida AB, Hardingham TE. Human infrapatellar fat pad-derived stem cells express the pericyte marker 3G5 and show enhanced chondrogenesis after expansion in fibroblast growth factor-2. Arthritis Res Ther 2008;10:R74.
27. Sengenes C, Lolmede K, Zakaroff-Girard A, Busse R, Bouloumie A. Preadipocytes in the human subcutaneous adipose tissue display distinct features from the adult mesenchymal and hematopoietic stem cells. J Cell Physiol 2005;205:114–122.
28. Astori G, Vignati F, Bardelli S, Tubio M, Gola M, Albertini V, Bambi F, Scali G, Castelli D, Rasini V, Soldati G, Moccetti T. "In vitro" and multicolor phenotypic characterization of cell subpopulations identified in fresh human adipose tissue stromal vascular fraction and in the derived mesenchymal stem cells. J Transl Med 2007;5:55.
29. Suga H, Matsumoto D, Eto H, Inoue K, Aoi N, Kato H, Araki J, Yoshimura K. Functional implications of CD34 expression in human adipose-derived stem/progenitor cells. Stem Cells Dev (in press).
30. Donnenberg VS, Landreneau RJ, Donnenberg AD. Tumorigenic stem and progenitor cells: Implications for the therapeutic index of anti-cancer agents. J Control Release 2007;122:385–391.
31. Donnenberg AD. Statistics of immunological testing. In: O'Gorman MR, Donnenberg AD, editors. Handbook of human immunology, 2nd ed. Boca Raton: CRC Press Taylor and Francis; 2008. p 29–62.
32. Fina L, Molgaard HV, Robertson D, Bradley NJ, Monaghan P, Delia D, Sutherland DR, Baker MA, Greaves MF. Expression of the CD34 gene in vascular endothelial cells. Blood 1990;75:2417–2426.
33. Baum CM, Weissman IL, Tsukamoto AS, Buckle AM, Peault B. Isolation of a candidate human hematopoietic stem-cell population. Proc Natl Acad Sci USA 1992;89:2804–2808.
34. Craig W, Kay R, Cutler RL, Lansdorp PM. Expression of Thy-1 on human hematopoietic progenitor cells. J Exp Med 1993;177:1331–1342.
35. Young HE, Steele TA, Bray RA, Hudson J, Floyd JA, Hawkins K, Thomas K, Austin T, Edwards C, Cuzzourt J, Duenzl M, Lucas PA, Black AC Jr. Human reserve pluripotent mesenchymal stem cells are present in the connective tissues of skeletal muscle and dermis derived from fetal, adult, and geriatric donors. Anat Rec 2001;264:51–62.
36. Jones EA, Kinsey SE, English A, Jones RA, Straszynski L, Meredith DM, Markham AF, Jack A, Emery P, McGonagle D. Isolation and characterization of bone marrow multipotential mesenchymal progenitor cells. Arthritis Rheum 2002;46:3349–3360.
37. Mason JC, Yarwood H, Tarnok A, Sugars K, Harrison AA, Robinson PJ, Haskard DO. Human Thy-1 is cytokine-inducible on vascular endothelial cells and is a signaling molecule regulated by protein kinase C. J Immunol 1996;157:874–883.
38. Saalbach A, Wetzig T, Haustein UF, Anderegg U. Detection of human soluble Thy-1 in serum by ELISA. Fibroblasts and activated endothelial cells are a possible source of soluble Thy-1 in serum. Cell Tissue Res 1999;298:307–315.
39. Rajkumar VS, Howell K, Csiszar K, Denton CP, Black CM, Abraham DJ. Shared expression of phenotypic markers in systemic sclerosis indicates a convergence of pericytes and fibroblasts to a myofibroblast lineage in fibrosis. Arthritis Res Ther 2005;7:R1113–R1123.
40. Sperr WR, Bankl HC, Mundigler G, Klappacher G, Grossschmidt K, Agis H, Simon P, Laufer P, Imhof M, Radaszkiewicz T, Glogar D, Lechner K, Valent P. The human cardiac mast cell: Localization, isolation, phenotype, and functional characterization. Blood 1994;84:3876–3884.
41. Donnenberg AD, Donnenberg VS. Rare-event analysis in flow cytometry. Clin Lab Med 2007;27:627–652, viii.
42. Mobius-Winkler S, Hollriegel R, Schuler G, Adams V. Endothelial progenitor cells: Implications for cardiovascular disease. Cytometry Part A 2009;75A:25–37.
43. Middleton J, Americh L, Gayon R, Julien D, Mansat M, Mansat P, Anract P, Cantagrel A, Cattan P, Reimund JM, Aguilar L, Amalric F, Girard JP. A comparative study of endothelial cell markers expressed in chronically inflamed human tissues: MECA-79, Duffy antigen receptor for chemokines, von Willebrand factor, CD31, CD34, CD105 and CD146. J Pathol 2005;206:260–268.
44. Both SK, van der Muijsenberg AJ, van Blitterswijk CA, de Boer J, de Bruijn JD. A rapid and efficient method for expansion of human mesenchymal stem cells. Tissue Eng 2007;13:3–9.
45. Lee SY, Lim J, Khang G, Son Y, Choung PH, Kang SS, Chun SY, Shin HI, Kim SY, Park EK. Enhanced ex vivo expansion of human adipose tissue-derived mesenchymal stromal cells by fibroblast growth factor-2 and dexamethasone. Tissue Eng Part A 2009;15:2491–2499.
46. Hutley LJ, Herington AC, Shurety W, Cheung C, Vesey DA, Cameron DP, Prins JB. Human adipose tissue endothelial cells promote preadipocyte proliferation. Am J Physiol Endocrinol Metab 2001;281:E1037–E1044.
47. Frye CA, Wu X, Patrick CW. Microvascular endothelial cells sustain preadipocyte viability under hypoxic conditions. In Vitro Cell Dev Biol Anim 2005;41(5/6):160–164.
48. Farrington-Rock C, Crofts NJ, Doherty MJ, Ashton BA, Griffin-Jones C, Canfield AE. Chondrogenic and adipogenic potential of microvascular pericytes. Circulation 2004;110:2226–2232.